A coupling model for solid-state anaerobic digestion in leach-bed reactors: Mobile-Immobile water and anaerobic digestion model

A. Coutu, M.A. Hernández-Shek, S. Mottelet, S. Guérin, V. Rocher, A. Pauss, T. Ribeiro

A coupling model for solid-state anaerobic digestion in leach-bed reactors: Mobile-Immobile water and anaerobic digestion model

A. Coutu[a], M. A. Hernández-Shek[a], S. Mottelet[b], S. Guérin[c], V. Rocher[c], A. Pauss[b], T. Ribeiro[a*]

[a]Institut Polytechnique UniLaSalle, Université d'Artois, ULR 7519, 19 Rue Pierre Waguet, BP 30313, 60026 Beauvais, France.

[b]Université de Technologie de Compiègne, ESCOM, TIMR (Integrated Transformations of Renewable Matter), Centre de recherche Royallieu - CS 60 319 - 60 203 Compiègne Cedex

[c]Direction Innovation SIAAP – Service public pour l'assainissement francilien, 82 avenue Kléber 92 700 Colombes, France

*Corresponding author: Thierry Ribeiro; Tel.: +33 (0) 344 06 76 11; E-mail: thierry.ribeiro@unilasalle.fr

Abstract

A coupling distributed solid-state anaerobic digestion model was developed and performed considering a simplified AM2 model and a saturated Mobile-Immobile water Model (MIM). This model allows considering both microporosity and macroporosity evolutions as well as the impact on biological kinetics. This model was adapted, implemented and validated on cattle manure in mesophilic conditions and carried out in a solid-state leach-bed reactor. Three 60L sacrificial leach-bed reactors were used to determine hydrodynamics and kinetic parameters in a calibration-validation approach. A sensitivity analysis was conducted and has shown a high value of hydrolysis kinetics on outputs variables (until 92% for accumulated methane yield and 72% for volatile fatty acids accumulation) which confirmed the necessity to identify accurately the hydrolysis parameter before calibration step. Finally, the solutes present inside each mobile and immobile region evolved in a different way confirming the model relevance.

Keywords

Biogas; Mathematical modeling; Sensitivity analysis; Porosity; kinetic parameters

1 Introduction

Anaerobic digestion (AD) is a biological process which consists of biodegradation of one or several organic substrates by a microbial consortium to produce biogas and digestate. This biogas is mainly composed of methane, carbon dioxide with few hydrogen sulfides. This biomethane is a renewable energy that can be valorized by injection or by cogeneration of heat and electricity. The digestate is a mixture of compounds of difficult degradation and mineral substances (Deublein, 2010). For 30 years, the global warning consciousness and increased energy prices have stimulated development of AD technology to produce energy from different substrates. In Europe, more than 18 200 units were recorded at the end of 2018. Electricity generated by cogeneration from biogas reached 63.5 TWh and the biomethane injected into the natural gas network represented 22.78 TWh (EBA, 2019). This process has many advantages: production of renewable energy through the fermentable waste treatment, with a double valorization of organic matter and energy (Kamali et al., 2016) and a reduction in greenhouse gas emissions by substituting fossil fuels and chemical fertilizers. Two types of AD process exist depending on the total solid content (TS): the liquid AD and the solid-state anaerobic digestion (SS-AD). The SS-AD is defined by a solid content higher than 15 % and is more appropriate for degradation of substrates with varying composition and high solid content (Degueurce et al., 2016; André et al., 2018; Rocamora et al., 2020). This last one allows a reduced need of water and a higher production rate (Brummeler et al., 2000) but only represents 9 % of the installed agricultural units and the main substrates are pig and cattle manure, cereals waste, corn silage, vegetables and plants wastes (ADEME, 2013; André et al., 2018). Numerous scientific and technological hurdles are present in SS-AD and limit the development of the process: biochemical methane potential, monitoring tools, Inoculum properties, hydrodynamics, rheology, codigestion and inhibition, pretreatments, dynamic of populations and conception (André et al., 2018).

A mathematical model is a tool that mainly represents the biological kinetics and physical behavior using equations. Several objectives are reachable: quantifying and simulate the system (Pastor-Poquet et al., 2019), understanding of the phenomenon (Fdez-Güelfo et al., 2011; Du et al., 2021) or prediction and control tool (Donoso-Bravo, 2011; Zhou et al., 2020). Many modified and advanced SS-AD model exist respecting essentially 3 ways of proceeding. The first way (1) is the modeling of perfectly mixed systems using "macro" parameters to consider the modulation of kinetic parameters with respect to the spatialization of the phenomena. In this first category are the simplest models for anaerobic digestion modeling: the first-order kinetics. These models consider the evolution of each component with a first-order kinetic to quickly modeling methane production or hydrolysis step (El-Mashad and Zhang, 2010; Kafle and Kim, 2011; Dennehy et al., 2016; Kouas et al., 2018). These models are easy to implement with few parameters to identify. More developed models like Gompertz model or dual-pooled first order kinetic model exist in literature considering several substrates, high volatile fatty acids content (Rao et al., 2000; Xie et al., 2011; Dennehy et al., 2016) or acclimatization and growth rate of biomass (Velázquez-Martí et al., 2019). A wide range of other models dealing with anaerobic digestion exist. More detailed and extended models using ordinary differential equation systems were developed to consider the complexity of anaerobic digestion phenomenon considering reaction network, physical and chemical equilibria, and hydrodynamics such as ADM1, AM2, AM2HN and their variants (Bernard et al., 2001; Batstone et al., 2002; Federovich et al., 2003; Ramirez et al., 2009; Sbarciog et al., 2010; Bollon et al., 2011; Abbassi-Guendouz et al., 2012; Benyahia et al., 2012; Donoso-Bravo et al., 2015; Liotta et al., 2015). The two-particle model consider SS-AD to be heterogeneous and postulate the existence of two particles types inside the solid matter named "seed" and "waste" particles (Kalyuzhnyi et al., 2000). Seed particles represent inoculum and waste particles are substrates. This model includes diffusion of solutes phenomenon between particles using the Fick law. The reaction front model (Martin et al., 2003) allows to describe poor seeding situations when there are spatial

separations between acidogenic and methanogenic zones considering a “reaction front” composed by layers. While these models are usually adequate to describe anaerobic digestion in perfectly stirred tank reactors or plug-flow reactors, the spatialization is not considered inside the reactor. The second way (2) of proceeding is to approximate spatialization using a set of simple models interconnected. It is the case of gradostat models essentially consisting of a set of two or more interconnected steady-state reactors called chemostats (Smith and Waltman, 1995; Harmand et al., 2017; Rapaport, 2018) with two-way flow between them and input and output at either end (Lovitt and Wimpenny, 1981). The design of chemical reactors has been studied for decades (Froment et al., 2010) and many optimizations were done on the design and operations of chemostats and gradostats (Zambrano and Carlsson, 2014; Zambrano et al., 2015; Bayen and Gajado, 2019; Crespo and Rapaport, 2020; Taylor and Rapaport, 2021). Finally, the last way (3) to describe anaerobic digestion is to write down complex systems of partial differential equation system (PDES) following mass balance. These distributed models are much less chosen by authors to describe SS-AD probably due to mathematical difficulty and identification issues. However, several promising research directions for SS-AD were developed and resumed by Xu et al (2015). The main PDES models for SS-AD are the distributed model (Vavilin et al., 2003; Vavilin et al., 2004; Vavilin et al., 2005; Vavilin et al., 2007; Vavilin et al., 2008), the spatio-temporal model and the diffusion-limitation model considering mass transfer by leachate flow and diffusion. These models use partial differential equations and include both time and spatial variations. The diffusion limitation model is combining the reaction front and the two-particle model (Xu et al., 2014) and the spatial-temporal model is a mathematical generalization of the distributed model and the reaction front in a 3-D regime (Eberl et al., 2003; Eberl et al., 2005). Numerous physical phenomena have been considered in those models but there is still a lack of knowledge of the cohesion between the porosity modification, hydric transfers and the dynamic of microbial populations, in particular with SS-AD model. In fact, recent studies (André et al., 2015, Shewani et al., 2015) have

shown that permeability, bulk and dry density evolution during SS-AD induced waste structure changes impacting the recirculation flow and biogas production.

In the present work, the first objective was to mathematically develop an innovative 1-D distributed model with leachate recirculation considering the macroporosity and the microporosity evolution during SS-AD. For this purpose, a simplified three-reaction mechanistic model kinetic model (Donoso-Bravo et al., 2015) and a saturated Mobile-IMmobile water model (MIM) (van Genuchten and Wierenga, 1976) were combined to consider respectively biokinetics and porosity hydrodynamics. The second objective was to adapt, implement and validate this model on cattle manure in mesophilic conditions in a homogeneous leach-bed reactor with a calibration-validation method.

2 Materials and methods

2.1 Physicochemical characterization of substrate and inoculum used

Cattle manure (CM) was chosen as substrate to compare hydrodynamic parameters obtained with existing data (André et al., 2015). CM was sampled from the farm of the UniLaSalle Polytechnic Institute (Beauvais, France). Used CM did not undergo any preliminary treatment. The liquid part of the manure (i.e. liquid bovin manure (LM)) was used as *inoculum* to bring the microbial consortium.

All the analyses were carried out in triplicate. The total solid content (TS), the volatile solid (VS) of the *inoculum*, CM and DG were determined by a 105°C drying for 24h and a combustion at 550°C for 2h (APHA, 1988). The pH of the *inoculum* was determined using a pH meter (Mettler Toledo, Switzerland). The total volatile fatty acid content (VFA) and the buffer capacity (TAC) were determined by two titrations using sulfuric acid with an automatic titrator (Mettler Toledo, Switzerland). The VFA value allowed to determine the volatile fatty acids quantity inside the

120 inoculum. Finally, the biochemical methane potential (BMP) was measured using an AMPTS I
121 device (Automatic Potential Test System, Bioprocess Control, Sweden) according to Holliger et al.
122 (2016). These tests were conducted at the beginning the experiments and the results are
123 illustrated in **Table 1**.

124 *2.2 Experimental set-up*

125 Three leach-bed reactors (LBR) made of polyethylene with a total volume of 60 L (considering a 50
126 cm height and a 39 cm diameter) were used. These reactors were divided into two parts: the upper
127 part containing the solid phase and the bottom part containing the liquid phase. These parts were
128 separated by a mesh performed with holes of 5 mm diameter to avoid solid blockages in the
129 recirculation pipe. Each reactor had a liquid recirculation. Approximately 40 L of liquid phase were
130 daily recirculated during 2 min each 2 h with a 100 $L.h^{-1}$ flow rate using peristaltic pumps
131 (Masterflex, USA). Thus, the liquid phase was spread out across the top of the solid phase in the
132 LBR and percolated to drop back into the bottom part. The top of the reactor was directly
133 connected with biogas flow counters (Drum gas meter TG5 Ritter, Germany) and biogas production
134 was continually measured. The biogas composition (CH_4, CO_2, H_2) was daily monitored by a biogas
135 analyzer (MGA300 multi-gas analyser ADC gas analysis Ltd., Hoddesdon United Kingdom).

136 At the beginning of the experiment, three LBR were simultaneously launched in the same
137 experimental conditions as illustrated in **Fig 1**. 21 kg of CM were placed inside each reactor with 22
138 kg of *inoculum* (LM) to obtain a ratio *inoculum*/substrate (I/S) of VS content equal to 0.05. The I/S =
139 0.05 ratio was chosen to increase methane productivity with a very low risk of reactor failure due
140 to VFA accumulation (Rouches et al., 2019). Moreover, it is a standard order of magnitude used in
141 solid-state anaerobic digestion (André et al., 2019; Hernandez-Shek et al., 2020). These reactors
142 were then hermetically sealed and the temperature was held at a constant value of 37°C with a
143 thermostatically controlled water bath for each reactor. These LBR were then sacrificed at different

144 stages of SS-AD. The first reactor was sacrificed during the first methane production peak on the
145 10th day after launching (R1), the second was sacrificed after the second methane production peak
146 during the 21th day (R2), and the last one at the end of SS-AD (R3) (when biogas flow is lower than
147 a 1% variation). At the end of each experiment, mass balances were determined for the three LBR.
148 The first 15 days were used to calibrate and the last 15 days were used to validate the kinetic
149 parameters. LBR were sacrificed to determine the raw material degradation as a function of time
150 and the experimental standard deviation on accumulated methane yield and VFA production.

151 ### *2.3 Mathematical model implementation*

152 A simplified biological kinetic three-reaction mechanistic model scheme was used for this study,
153 updated with hydric transfers equations of the MIM model.

154 #### *2.3.1 Anaerobic digestion model and reaction kinetics*

155 The simplified three-reaction mechanistic model used was inspired by the model described in
156 Donoso-Bravo et al. (2015). Some assumptions have been done to guarantee the model usefulness.
157 The following hypothesis were considered: (1) All the variables were measured on a COD basis. (2)
158 The main macromolecular compounds (carbohydrates, proteins and lipids) were grouped into one
159 generic compound. (3) Instead of a pool of volatile fatty acids, only a generic equivalent acetic acid
160 was considered (Bernard *et al.*, 2001). These considerations were convenient for reducing the
161 number of parameters to be determined. As a consequence, the acetogenesis was suppressed
162 from the model. (4) Ammonia was not considered. (5) Hydrogen was not considered in the model.
163 (6) the methane solubility was neglected. The three following biochemical equations (1), (2) and (3)
164 represent this model:

Hydrolysis $S_0 \xrightarrow{r_0} S_1$ **(1)**

Acidogenesis $$S_1 \xrightarrow{r_1} Y_{X1}X_1 + (1 - Y_{X1})S_2$$ **(2)**

Methanogenesis $$S_2 \xrightarrow{r_2} Y_{X2}X_2 + (1 - Y_{X2})CH_4$$ **(3)**

The CO_2 does not appear in these equations because it represents obviously a COD zero balance. S_0 represents the raw substrate, S_1 the hydrolyzed substrate, S_2 the generic equivalent of volatile fatty acids and CH4 is the accumulated methane yield. X_1 and X_2 are respectively the acidogenic and methanogenic biomasses and Y_{X1} and Y_{X2} the associated growth rate. Concerning the reaction kinetics, the hydrolysis was represented by a classic first-order equation to decrease the number of parameters (Vavilin et al., 2008; Batstone et al., 2009). A Monod kinetic was used for acidogenesis and a Haldane kinetic for methanogenesis, allowing to consider an inhibition parameter concerning the acid concentration for the accumulated methane yield. A Peterson matrix summarizes these kinetics **Table 3**.

2.3.2 Hydrodynamics modeling

Several mass transfer experimental studies in sorbing porous media (Coats and Smith, 1964; van Genuchten and Wieranga, 1976; Abulaban et al., 1998; Zhou and Selim, 2001; Kolchanova et al., 2022) indicated that liquid percolation is modified when the pore water porosity changes. The first model of a solute in porous media considering diffusion and dispersion phenomena in 1-D dimension was the convective-dispersive equation (Lapidus and Amundson, 1952). This model is described by the following equation (4).

$$\frac{\partial C(z,t)}{\partial t} = D\frac{\partial^2 C(z,t)}{\partial z^2} - \vartheta_0 \frac{\partial C(z,t)}{\partial z} \quad (4)$$

Where C is the solute concentration inside the sorbing porous media ($kg.m^{-3}$), D is the diffusion coefficient ($m^2.h^{-1}$), z is the distance (m) and ϑ_0 is the pore-water velocity ($m.h^{-1}$). This model was modified to include transfer by diffusion from dynamic flowing regions to immobile zones with the

model described by Coats and Smith (1964) and expanded Deans' (1963) model illustrated in equations (5) and (6). This model is called two-region model, known as MIM (M-mobile/IM-immobile water).

$$\theta_m \frac{\partial C_m(z,t)}{\partial t} + \theta_{im} \frac{\partial C_{im}(z,t)}{\partial t} = \theta_m D \frac{\partial^2 C_m(z,t)}{\partial z^2} - \vartheta_m \theta_m \frac{\partial C_m(z,t)}{\partial z} \quad \textbf{(5)}$$

$$\theta_{im} \frac{\partial C_{im}(z,t)}{\partial t} = \alpha (C_m(z,t) - C_{im}(z,t)) \quad \textbf{(6)}$$

Where θ_m and θ_{im} are the fractions of solid matter filled with mobile and immobile water ($m^3_{solute}.m^{-3}$). C_m and C_{im} are the solute concentrations in mobile and immobile regions ($kg.m^{-3}$), ϑ_m is the average pore-water velocity in the mobile part and α is the mass transfer coefficient between mobile and immobile regions. These equations do not consider any chemical or biological reactions. Moreover, some simplifications were done to adapt the transfer between the two regions with current equations. Following the general transport equation (van Genuchten and Wieranga, 1976), it was possible to adapt these equations for SS-AD for each region as represented in equations (7) and (8):

$$\frac{\partial}{\partial t}(\theta_m(t) C_m(z,t)) + \frac{\partial}{\partial t}(\theta_{im}(t) C_{im}(z,t)) + \frac{\partial}{\partial t}(f \rho S_m(z,t)) + \frac{\partial}{\partial t}(1-f)\rho S_{im}(z,t) = \frac{\partial}{\partial z}\left(\theta_m(t) D \frac{\partial C_m(z,t)}{\partial z}\right) - \frac{\partial}{\partial z}(q C_m(z,t)) \quad \textbf{(7)}$$

$$\frac{\partial}{\partial t}(\theta_{im}(t) C_{im}(z,t)) + (1-f)\rho \frac{\partial S_{im}(z,t)}{\partial t} = \alpha (C_m(z,t) - C_{im}(z,t)) \quad \textbf{(8)}$$

Where f is the fraction of sorption sites which are in contact with the mobile region, q is the darcian velocity ($m.h^{-1}$) and ρ is the bulk density ($kg.m^{-3}$). S_m and S_{im} are the sorbed concentrations of solute ($kg_{solute}.kg^{-1}$). In the model considered, sorption phenomenon was not considered. Therefore, the equations (7) and (8) became the following equations (9) and (10):

$$\frac{\partial}{\partial t}(\theta_m(t)C_m(z,t)) + \frac{\partial}{\partial t}(\theta_{im}(t)C_{im}(z,t)) = \frac{\partial}{\partial z}\left(\theta_m(t)D\frac{\partial C_m(z,t)}{\partial z}\right) - \frac{\partial}{\partial z}(qC_m(z,t)) \quad \textbf{(9)}$$

$$\frac{\partial}{\partial t}(\theta_{im}(t)C_{im}(z,t)) = \alpha(C_m(z,t) - C_{im}(z,t)) \quad \textbf{(10)}$$

The concentrations were expressed in $kg_{COD}.m^{-3}$ for the model used. It was assumed that fractions of solid matter filled with mobile and immobile water were function of time. Moreover, the diffusion coefficient D and the water flux represented by the darcian velocity were considered constants over time and space. The fraction of solid matter in each region was supposed independent of the distance z. The equations (9) and (10) became (11) and (12):

$$\theta_m(t)\frac{\partial}{\partial t}C_m(z,t) + C_m(z,t)\frac{\partial}{\partial t}\theta_m(t) + \alpha(C_m(z,t) - C_{im}(z,t)) = \theta_m(t)D\frac{\partial^2 C_m(z,t)}{\partial z^2} - q\frac{\partial C_m(z,t)}{\partial z} \quad \textbf{(11)}$$

$$\theta_{im}(t)\frac{\partial}{\partial t}C_{im}(z,t) + C_{im}(z,t)\frac{\partial}{\partial t}\theta_{im}(t) = \alpha(C_m(z,t) - C_{im}(z,t)) \quad \textbf{(12)}$$

The equations (11) and (12) were used to describe the movement of each solute through the leach bed. It was also necessary to add a production term considering the biological kinetics of each solute that finally led to the model used. The hydrodynamics considerations for the model used are represented in **Fig 2**.

2.3.3 Model used

To obtain a functional model, kinetics terms had to be added to the previous equations for each solute in accordance with equations (11) and (12) and with the Hydrolysis consideration. The equations are presented for each solute considering each reaction respecting a global template in equations (13) and (14).

$$\theta_m(t)\frac{\partial}{\partial t}C_m^i(z,t) + C_m^i(z,t)\frac{\partial}{\partial t}\theta_m(t) + \alpha\left(C_m^i(z,t) - C_{im}^i(z,t)\right) = \theta_m(t)D(t)\frac{\partial^2 C_m^i(z,t)}{\partial z^2} - q\frac{\partial C_m^i(z,t)}{\partial z} + \theta_m(t)\sum_{j=1}^{M}\sigma_j r_m^j(z,t) \quad \textbf{(13)}$$

$$\theta_{im}(t)\frac{\partial}{\partial t}C_{im}^i(z,t) + C_{im}^i(z,t)\frac{\partial}{\partial t}\theta_{im}(t) = \alpha\left(C_m^i(z,t) - C_{im}^i(z,t)\right) + \theta_{im}(t)\sum_{j=1}^{M}\sigma_j r_{im}^j(z,t) \quad \textbf{(14)}$$

Where i represents each solute, σ_j is the stoichiometric coefficient of each solute considered in the M reactions (j is the discrete variable for each reaction considered). The reaction rate for each reaction is r_m^j ($kg_{COD}.m^{-3}.d^{-1}$). Moreover, in these equations θ_m and θ_{im} are time-dependents and each reaction rate was depending on the region considered. The kinetics coefficients were still constant and the Peterson matrix is illustrated in **Table 4**. f_{m0} is the raw substrate degradation rate into the mobil region and (1-f_{m0}) is the raw substrate degradation rate into the immobile region. The model equations are presented in biochemical equations (15-19).

Hydrolysis $S_0 \xrightarrow{r_0} f_{m0}S_1^m + (1-f_{m0})S_1^{im}$ **(15)**

Acidogenesis

Mobile region $S_1^m \xrightarrow{r_1^m} Y_{X1}X_1^m + (1-Y_{X1})S_2^m$ **(16)**

Immobile region $S_1^{im} \xrightarrow{r_1^{im}} Y_{X1}X_1^{im} + (1-Y_{X1})S_2^{im}$ **(17)**

Methanogenesis $S_2^m \xrightarrow{r_2^m} Y_{X2}X_2^m + (1-Y_{X2})CH_4$ **(18)**

Mobile region

Immobile region $S_2^{im} \xrightarrow{r_2^{im}} Y_{X2}X_2^{im} + (1-Y_{X2})CH_4$ **(19)**

f_{m0} was considered equal to 0 because raw substrate was supposed hydrolyzed only in the immobile region. In fact, only raw substrate directly in contact with leachate could be hydrolyzed

and the immobile region is considered as the liquid part directly in contact with raw substrate. Equations (13) and (14) consider spatial and temporal variations and represented the simplified three-reaction mechanistic model and MIM distributed model for each solute. In this study, the LBR content was supposed homogeneous and depended exclusively on time as only one substrate was used and the LBR size was too small to have a compaction effect on cattle manure. Then equations (13) and (14) become (20) and (21).

$$\theta_m(t)\frac{\partial}{\partial t}C_m^i(t) + C_m^i(t)\frac{\partial}{\partial t}\theta_m(t) + \alpha\left(C_m^i(t) - C_{im}^i(t)\right) = \sum_{j=1}^{M}\sigma_j r_m^j(t) \quad \textbf{(20)}$$

$$\theta_{im}(t)\frac{\partial}{\partial t}C_{im}^i(t) + C_{im}^i(t)\frac{\partial}{\partial t}\theta_{im}(t) = \alpha\left(C_m^i(t) - C_{im}^i(t)\right) + \sum_{j=1}^{M}\sigma_j r_{im}^j(t) \quad \textbf{(21)}$$

2.3.4 Differential equations system

The system was composed of 10 differential equations (ODE) and 10 state variables ($S_0, S_1^m, S_1^{im}, S_2^m, S_2^{im}, X_1^m, X_1^{im}, X_2^m, X_2^{im}, CH_4$). All the kinetics rates were studied in mesophilic conditions and expressed supra. Now considering each solute:

- Raw substrate S_0:

$$\frac{d}{dt}S_0(t) = -\mathrm{r}_0 \quad \textbf{(22)}$$

The raw substrate was in a solid form only and its degradation was supposed homogeneous. This is a first order equation and it could be directly solved to obtain μ_0 :

$$\frac{d}{dt}S_0(t) = -\mu_0 S_0(t) \Leftrightarrow \mu_0 = \frac{-1}{\Delta t} ln\left(\frac{S_0^f}{S_0^0}\right) \quad \textbf{(23)}$$

Δt is the experiment duration, S_0^0 is the initial raw substrate concentration and S_0^f the final raw substrate concentration.

- Hydrolyzed substrate S_1:

$$\theta_m(t)\frac{d}{dt}S_1^m(t) + S_1^m(t)\frac{d}{dt}\theta_m(t) + \alpha\left(S_1^m(t) - S_1^{im}(t)\right) = -\theta_m(t)r_1^m(t) \quad \textbf{(24)}$$

$$\theta_{im}(t)\frac{d}{dt}S_1^{im}(t) + S_1^{im}(t)\frac{d}{dt}\theta_{im}(t) = \alpha\left(S_1^m(t) - S_1^{im}(t)\right) + r_0(t) \quad \textbf{(25)}$$

The hydrolyzed substrate was produced by a hydrolysis step and consumed by an acidogenesis step. Hydrolysis was supposed to be a contact reaction and considered in the immobile region only. Reaction rates for the other reactions were considered in the mobile region only. This assumption was done in accordance with literature (Abbassi-Guendouz et al., 2012; Shewani et al., 2015; Hernandez-Shek et al., 2020): assuming that the intrinsic activity of the microbial consortium was considered inversely proportional to the TS content.

- Volatile fatty acids S_2:

$$\theta_m(t)\frac{d}{dt}S_2^m(t) + S_2^m(t)\frac{d}{dt}\theta_m(t) + \alpha\left(S_2^m(t) - S_2^{im}(t)\right) = \theta_m(t)[(1 - Y_{X1})r_1^m(t) - r_2^m(t)] \quad \textbf{(26)}$$

$$\theta_{im}(t)\frac{d}{dt}S_2^{im}(t) + S_2^{im}(t)\frac{d}{dt}\theta_{im}(t) = \alpha\left(S_2^m(t) - S_2^{im}(t)\right) \quad \textbf{(27)}$$

The volatile fatty acids were produced by acidogenesis step and consumed by methanogenesis step. The reactions were considered in each region separately and the mass transfer was supposed not to be affected by other solutes.

- Acidogenic biomass X_1:

$$\theta_m(t)\frac{d}{dt}X_1^m(t) + X_1^m(t)\frac{d}{dt}\theta_m(t) + \alpha\left(X_1^m(t) - X_1^{im}(t)\right) = \theta_m(t)Y_{X1}r_1^m(t) \quad \textbf{(28)}$$

$$\theta_{im}(t)\frac{d}{dt}X_1^{im}(t) + X_1^{im}(t)\frac{d}{dt}\theta_{im}(t) = \alpha\left(X_1^m(t) - X_1^{im}(t)\right) \quad \textbf{(29)}$$

The acidogenic biomass was produced by the acidogenesis step but the biomass decay was not considered to simplify and minimize the number of parameters.

- Methanogenic biomass X_2:

$$\theta_m(t)\frac{d}{dt}X_2^m(t) + X_2^m(t)\frac{d}{dt}\theta_m(t) + \alpha\left(X_2^m(t) - X_2^{im}(t)\right) = \theta_m(t)Y_{X2}r_2^m(t) \quad \textbf{(30)}$$

$$\theta_{im}(t)\frac{d}{dt}X_2^{im}(t) + X_2^{im}(t)\frac{d}{dt}\theta_{im}(t) = \alpha\left(X_2^m(t) - X_2^{im}(t)\right) \quad \textbf{(31)}$$

The methanogenic biomass was produced by the methanogenesis step but the biomass decay was still not considered.

- Accumulated methane yield CH_4:

$$\frac{d}{dt}CH_4(t) = (1 - Y_{X2})\left(\theta_m(t)r_2^m(t)\right) \quad \textbf{(32)}$$

The methane was produced by methanogenesis step and in each mobile and immobile region. The methane solubility was neglected. As a consequence, the gaseous methane was directly considered in this equation. The differential equations systems to solve were equations (22-32). Concerning initial conditions, the volatile fatty acids, hydrolyzed solute and biomasses were supposed to be present only in the mobile region, because these compounds were added by *inoculum* presence. The raw substrate was considered uniform across the LBR length. These initial conditions are represented by the following equations (33):

$$S_0(t_0) = S_0^0, S_1^m(t_0) = 0, S_1^{im}(t_0) = 0, S_2^m(t_0) = \frac{S_2^0}{\theta_m}, S_2^{im}(t_0) = 0,$$

$$X_1^m(t_0) = \frac{X_1^0}{\theta_m}, X_1^{im}(t_0) = 0, X_2^m(t_0) = \frac{X_2^0}{\theta_m}, X_2^{im}(t_0) = 0, CH_4(t_0) = 0 \quad \textbf{(33)}$$

All solute components were initially supposed being in the mobile region only.

2.4 *Hydrodynamic parameters used*

Hydrodynamic parameters θ_m, θ_{im} representing the fractions of solid matter filled with mobile and immobile water inside the leach-bed ($m^3_{solute}.m^{-3}$) were obtained from other SS-AD experiments on cattle manure. The measurement method used was following the method proposed by Hernandez-Shek (2020): the water retention curve (WRC) analysis. Each studied sample was immersed and saturated with water. The sample was then drained during 2 hours and residual water was evaporated using thermogravimetry. The different volumetric fractions obtained represented microporosity and macroporosity evolution over time. Each sample was studied in triplicates to ensure representativeness of proposed methodology. These fractions were measured weighing total and added water from CM. These parameters were obtained at day 0, day 9, day 13, day 19 and day 31. α was found in the literature (André et al., 2015). The results obtained are illustrated in **Table 2**.

The biological kinetics occurred in liquid part so the total dry porosity θ was considered constant and equal to 100 % in the model. The mobile and immobile dry porosity θ_m and θ_{im} were modified considering these hypotheses. The solute exchange rate α was supposed to be constant and equal to $3.78.10^{-2}$ min^{-1} according to André et al. (2015). Regarding the mobile and immobile dry porosities, a linear regression was done to obtain an estimation of the parameters time dependencies. These regressions allowed to describe the time dependencies of θ_m, θ_{im} and α during the SS-AD as equations (34-35).

Mobile dry porosity	$\theta_m = -1.02.10^{-2}\mathrm{t} + 0.3208$	$R^2 = 0.987$	**(34)**
Immobile dry porosity	$\theta_{im} = 1.02.10^{-2}\mathrm{t} + 0.6792$	$R^2 = 0.987$	**(35)**

2.5 Computational aspects

2.5.1 Model calibration and validation

The model resolution, calibration and validation, and the sensitivity analysis were performed with Matlab R2019b. The optimization procedure to determine parameters values was done with the fmincon function. This function computes the minimum of a given function to perform the optimization of a non-linear optimization problem with constraints. Model calibration and validation were conducted on 2 different sets of data. The parameters determined by calibration part had to be validated with different data to ensure the model robustness. For parameters estimation, three experimental data were used: accumulated CH_4 yield, CH_4 flow and VFA concentration. The simulated CH_4 flow expression is described in equation (36). The parameters were estimated using a least-squares criterion minimizing the equation (37).

$$Q_{CH4}^{sim}(\mathrm{d}) = \frac{(CH_4(t_d) - CH_4(t_{\mathrm{d}-1}))}{(t_d - t_{\mathrm{d}-1})} \quad \textbf{(36)}$$

$$J(\theta_c) = \sigma_1 abs\left(CH_4^{exp} - CH_4^{sim}\right) + \sigma_2 abs\left(FOS_{exp} - \theta_m S_2^m - \theta_{im} S_2^{im}\right) + \sigma_3 abs\left(Q_{CH4}^{exp} - Q_{CH4}^{sim}\right) \quad \textbf{(37)}$$

With Q_{CH4}^{sim} the CH_4 flow simulated ($kg_{COD}.m^{-3}.d^{-1}$), Q_{CH4}^{exp} the experimental CH_4 flow ($kg_{COD}.m^{-3}.d^{-1}$), FOS_{exp} the experimental volatile fatty acids measurement ($kg_{COD}.m^{-3}$), CH_4^{sim} and CH_4^{exp} the accumulated methane yield measurement ($kg_{COD}.m^{-3}$). $\sigma_1, \sigma_2, \sigma_3$ are impact coefficients and represent the fraction of the objective function for each fitted variable, arbitrarily fixed and respectively equal to 0.5, 0.5 and 1. J is the objective function and θ_c the kinetic parameters to be determined.

2.5.2 *Initialization*

The kinetic parameters were initialized according to literature. **Table 5** describes all the values used for kinetic parameters initialization. Initialization values were obtained from Rakotoniaina (2012) and interval values from Müller et al. (2002) and Zaher et al. (2009) using the same substrate in mesophilic conditions (Simeonov et al., 1996).

2.5.3 *Model verification*

To validate the model used, a mass balance and a first simulation were led. The mass balance is expressed in (38) and verified in (39) with kinetics. Considering only liquid regions in this model, the total porosity was raised to 1. This is why the sum of θ_m and θ_{im} was considered equal to 1 to ensure the mass conservation in this mass balance. The fractions of solid matter filled with mobile and immobile water θ_m and θ_{im} were considered to conserve a common unit ($kg_{COD}.m^{-3}$):

$$Mass\ balance = S_0 + \theta_m(S_1^m + S_2^m + X_1^m + X_2^m) + \theta_{im}(S_1^{im} + S_2^{im} + X_1^{im} + X_2^{im}) + CH_4 \quad \textbf{(38)}$$

$$\frac{dS_0}{dt} + \frac{d\theta_m S_1^m}{dt} + \frac{d\theta_m S_2^m}{dt} + \frac{d\theta_m X_1^m}{dt} + \frac{d\theta_m X_2^m}{dt} + \frac{d\theta_{im} S_1^{im}}{dt} + \frac{d\theta_{im} S_2^{im}}{dt} + \frac{d\theta_{im} X_1^{im}}{dt} + \frac{d\theta_{im} X_2^{im}}{dt} + \frac{dCH_4}{dt} = 0 \quad \textbf{(39)}$$

The mass balance calculation was done respecting hydrodynamics assumptions described in **Fig 2**. The verification was done with initialization parameters. The different solute concentration behaviors between mobile and immobile regions legitimated the model benefit.

2.5.4 *Sensitivity analysis*

The state variable vector x (40) depended on time, on variables concentration and on model parameters p (40) as illustrated in equation (41). The model sensitivity is described by equation (42) and the equation to be solved was the equation (43).

$$x = \left(S_0, S_1^m, S_1^{im}, S_2^m, S_2^{im}, X_1^m, X_1^{im}, X_2^m, X_2^{im}, CH_4\right)$$

$$\text{and } p = (Y_{x1}, Y_{x2}, \mu_0, \mu_1^{max}, \mu_2^{max}, K_{S1}, K_{S2}, K_I) \quad \textbf{(40)}$$

$$\frac{\partial x}{\partial t} = f(t, x, p) \quad \textbf{(41)}$$

$$S(t) = \frac{\partial x}{\partial p} \quad \textbf{(42)}$$

$$\frac{\partial S(t)}{dt} = \frac{\partial f(t, x, p)}{\partial x} S + \frac{\partial f(t, x, p)}{\partial p} \quad \textbf{(43)}$$

The f function was known. Once the equation (41) was solved and the sensitivity matrix S was obtained, the sensitivity was known for each state variable against each parameter. These calculations were performed on the model using the kinetic parameters obtained from the calibration step and the hydrodynamics parameters obtained from experimental data. Calculations were done using complex-step derivative approximation method (Martin et al., 2003).

3 Results and discussion

3.1 Leach-bed reactor performance

For each experiment, mass balances were calculated. Mass balances were determined within a value range of 98.06% to 99.62% between the three LBR attesting the absence of local failures. The VS removal ranged from 25.76% to 52.29%. Results have shown optimal conditions with a great substrate accessibility. The accumulated methane yield, methane flow and VFA concentration are represented in **Fig 3**. The standard deviation between LBR were determined as a function of time between day 1 and day 21. After day 21 there was no more standard deviation calculation as only one LBR was still producing methane. 2 production peaks were observed at day 10 and day 15 and

a valley between these 2 production peaks represented a slack of methane production. This behavior was similar to the results commonly found in literature concerning SS-AD (André et al., 2015; Degueurce et al., 2016; Riggio et al., 2017). The accumulated methane yield reached 98.66% of the BMP measurement on day 28 and the volatile fatty acid content monitoring did not show any inhibition problems during these experiments. Experimental results have shown a great repeatability between each LBR, allowing to obtain representative results during calibration and validation steps.

3.2 Model calibration

The calibration of the kinetic parameters aimed to obtain the best fitting with the experimental results. Two different datasets were used for parameter estimation and validation: the average methane flow, the average accumulated methane yield and the average volatile fatty acid concentration before and after 15 days. The model calibration was carried out by trial and error in order to obtain a possible dataset. The first step was to determine the hydrolysis constant μ_0 with equation (132) using a linear regression on experimental solid phase COD measurements. A mean value of 0.04 d^{-1} was measured with R^2=0.97 and was the selected value for calibration step. LBR simulation results were close to the experimental data as represented in **Fig 3** until day 15. Experimental data are represented as red dots and simulated data are the blue lines. The calibrated parameters values obtained from the minimization procedure are presented in **Table 6**. Moreover, results were not obviously implausible: 9.28% of acidogenesis step COD consumption was used to feed acidogenic biomass and 23.76% of methanogenesis step COD consumption was used to feed methanogenesis biomass. This parameters combination was assumed not to be the unique possible combination.

3.3 Model validation

The developed model and parameters obtained during calibration step had to be validated with another dataset. The simulation obtained with calibration parameters correctly reproduced the behavior of the system for the complete period of 28 days as represented in **Fig 3**. The main quality of this model is its ability to predict the accumulated methane yield and VFA concentration behaviors with simple data, considering the porosity differences. However, the calibration is a very sensitive step and any process disturbance could modify the set of determined parameters. Asymptotic observers (Dochain et al., 1992) could not be used on this model as only global concentrations could be determined but not mobile and immobile regions concentrations. This is why each kinetic parameter was not identifiable but the global set of parameters could be approached. Moreover, the calibration step was sensitive to the initialization step. This is why a sensitivity analysis was necessary.

3.4 Sensitivity analysis

The global approach used for the minimization procedure posed 2 issues: a structural identifiability issue and a practical identifiability issue. In fact, the uniqueness of the parameters found could not be proved and local minima of the minimization of the global criterion in equation (37) could exist. This is why initialization step is very important and a sensitivity analysis was needed in this study. The sensitivity analysis was done considering accumulated methane yield, VFA concentration and methane flow rate as state variables. The studied parameters were kinetic parameters. The same curve shapes could be found for different of parameters. Monod and Haldane kinetic parameters sensitivities are illustrated in **Fig 4** for the methane flow. μ_1^{max} and K_{S1} (red curve and orange curve) have the same sensitivity behavior as well as μ_2^{max}, K_{S2} and K_I (green, purple and blue curves). This behavior was observed for each state variable. This meant that kinetic parameters were not identifiable with the available experimental data and the set of parameters obtained

during calibration step is assumed not to be the unique possible combination. **Fig 5** shows the absolute sensitivity of each output. The hydrolysis constant μ_0 was by far the most influential parameter for each output (until 92% for CH_4 yield (A) and 72% for VFA concentration (C) on **Fig 5**). This result confirmed that hydrolysis was considered as the limiting step in the reaction scheme and hydrolysis was a very important step for anaerobic digestion of cattle manure. Moreover, the acidogens and methanogens yields presented a high sensitivity for outputs, until 15% for accumulated CH_4 yield (A), 16% for CH_4 flow (B) and 77% for VFA concentration (C).

3.5 Hydrodynamics behavior of solutes

Solutes concentrations inside mobile and immobile regions are represented in **Fig 6**. These solutes present inside mobile and immobile regions evolved in a different way. Mobile region solutes had a higher concentration, probably due to the kinetic assumptions. Acidogenesis and methanogenesis biomasses seemed to accumulate faster and faster inside the immobile region, and were slower produced inside the mobile region. At the beginning of the experiment, solutes in mobile region quickly moved into the immobile region. This behavior was due to initial conditions hypothesis which consider no biomass in the immobile region before anaerobic digestion. This difference of solute behaviors between mobile and immobile regions spotlights the model relevance and could partially explain results observed in the literature concerning physical changes in the leach-bed during SS-AD of cattle manure (André et al., 2015; Shewani et al., 2015).

4 Conclusions

A distributed solid-state anaerobic digestion model considering the macroporosity and microporosity was mathematically developed and tested for a homogeneous leach-bed reactor using a simplified AM2 and a saturated Mobile-IMmobile water model. This model was adapted

and implemented for cattle manure SS-AD. This study provided a new understanding of hydrodynamics and macroporosity and microporosity differences impact on biokinetics. This model considered that microporosity increased proportionally to the macroporosity decrease inside the leach-bed as observed in literature. It could be very interesting to adapt this model for codigestion or implement this model for other substrates to observe the spatial heterogeneity effect.

5 Acknowledgments

The authors gratefully thank the program MOCOPEE (www.mocopee.fr) and the FEDER fund (FEDER PO Picardie / MOCOPEE PI0012581) for the support provided for this work and the PhD grant of Arnaud Coutu. The authors want to thank also Denis Dochain for his help, Laura André and Edvina Lamy for their technical help ; and Pauline Louis for her carefully reading of the manuscript.

6 References

Abbassi-Guendouz, A., Brockmann, D., Trably, E., Dumas, C., Delgenès, J.-P., Steyer, J.-P., Escudié, R., 2012. Total solids content drives high solid anaerobic digestion via mass transfer limitation. Bioresource Technology 111, 55–61. https://doi.org/10.1016/j.biortech.2012.01.174

Abulaban, A., Nieber, J.L., Misra, D., 1998. Modeling plume behavior for nonlinearly sorbing solutes in saturated homogeneous porous media. Advances in Water Resources 21, 487–498. https://doi.org/10.1016/S0309-1708(97)00007-9

ADEME, 2013. Estimation des gisements potentiels de substrats utilisables en methanisation. Available at https://www.ademe.fr/sites/default/files/assets/documents/88252_gisements-substrats-methanisation.pdf

André, L., Durante, M., Pauss, A., Lespinard, O., Ribeiro, T., Lamy, E., 2015. Quantifying physical structure changes and non-uniform water flow in cattle manure during dry anaerobic digestion process at lab scale: Implication for biogas production. Bioresource Technology 192, 660–669. https://doi.org/10.1016/j.biortech.2015.06.022

André, L., Pauss, A., Ribeiro, T., 2018. Solid anaerobic digestion: State-of-art, scientific and technological hurdles. Bioresour Technol 247, 1027–1037. https://doi.org/10.1016/j.biortech.2017.09.003

André, L., Zdanevitch, I., Pineau, C., Lencauchez, J., Damiano, A., Pauss, A., Ribeiro, T., 2019. Dry anaerobic co-digestion of roadside grass and cattle manure at a 60 L batch pilot scale. Bioresource Technology 289, 121737. https://doi.org/10.1016/j.biortech.2019.121737

APHA, 1998. Standard Methods for the Examination of Water and Wastewater. American Public Health Association, 20th ed. American water works association and water environment federation, Washington, USA.

Batstone, D.J., Keller, J., Angelidaki, I., Kalyuzhnyi, S.V., Pavlostathis, S.G., Rozzi, A., Sanders, W.T.M., Siegrist, H., Vavilin, V.A., 2002. The IWA Anaerobic Digestion Model No 1 (ADM1). Water Science and Technology 45, 65–73. https://doi.org/10.2166/wst.2002.0292

Batstone, D. j., Tait, S., Starrenburg, D., 2009. Estimation of hydrolysis parameters in full-scale anerobic digesters. Biotechnology and Bioengineering 102, 1513–1520. https://doi.org/10.1002/bit.22163

Bayen, T., Gajardo, P., 2019. On the steady state optimization of the biogas production in a two-stage anaerobic digestion model. J. Math. Biol. 78, 1067–1087. https://doi.org/10.1007/s00285-018-1301-3

Benyahia, B., Sari, T., Cherki, B., Harmand, J., 2012. Bifurcation and stability analysis of a two step model for monitoring anaerobic digestion processes. Journal of Process Control 22, 1008–1019. https://doi.org/10.1016/j.jprocont.2012.04.012

Bernard, O., Hadj-Sadok, Z., Dochain, D., Genovesi, A., Steyer, J.-P., 2001. Dynamical model development and parameter identification for an anaerobic wastewater treatment process. Biotechnology and Bioengineering 75, 424–438. https://doi.org/10.1002/bit.10036

Bollon, J., Le-hyaric, R., Benbelkacem, H., Buffiere, P., 2011. Development of a kinetic model for anaerobic dry digestion processes: Focus on acetate degradation and moisture content. Biochemical Engineering Journal 56, 212–218. https://doi.org/10.1016/j.bej.2011.06.011

Brummeler, E., 2000. Full scale experience with the BIOCEL process. Water Science and Technology 41, 299–304. https://doi.org/10.2166/wst.2000.0084

Coats, K. H., and Smith, B. D., 1964. Dead-end pore volumeEnd Pore Volume and Dispersion in Porous Media. Society of Petroleum Engineers Journal 4, 73–84. https://doi.org/10.2118/647-PA

Crespo, M., Rapaport, A., 2020. Analysis and dispersion in porous media. Soc. Pet. Eng.Optimization of the Chemostat Model with a Lateral Diffusive Compartment. J. 4:73-84 Journal of Optimization Theory and Applications 185, 597–621. https://doi.org/10.1007/s10957-020-01665-2

Deans, H. HA., 1963. A mathematical modelA Mathematical Model for dispersionDispersion in the direction of flow direction of flow in porous media. Porous Media. Society of Petroleum Engineers Journal 3, 49–52. https://doi.org/10.2118/493-PA

Degueurce A., Tremier A., Peu P., 2016. Dynamic effect of leachate recirculation on batch mode solid state anaerobic digestion: Influence of recirculated volume, leachate to substrate ratio and recirculation periodicity. Bioresource Technology 216, 553–561. https://doi.org/10.1016/j.biortech.2016.05.113

Dennehy, C., Lawlor, P.G., Croize, T., Jiang, Y., Morrison, L., Gardiner, G.E., Zhan, X., 2016. Synergism and effect of high initial volatile fatty acid concentrations during food waste and pig manure anaerobic co-digestion. Waste Management 56, 173–180. https://doi.org/10.1016/j.wasman.2016.06.032

Deublein D, Steinhauser A., 2010. Digested Residue in Biogas from Waste and Renewable Resources. John Wiley & Sons, Ltd, pp. 321–324. https://doi.org/10.1002/9783527632794.ch29

Dochain, D., Perrier, M., Ydstie, B.E., 1992. Asymptotic observers for stirred tank reactors. Chemical Engineering Science 47, 4167–4177. https://doi.org/10.1016/0009-2509(92)85166-9

Donoso-Bravo, A., Mailier, J., Martin, C., Rodríguez, J., Aceves-Lara, C.A., Wouwer, A.V., 2011. Model selection, identification and validation in anaerobic digestion: A review. Water Research 45, 5347–5364. https://doi.org/10.1016/j.watres.2011.08.059

Donoso-Bravo, A., Pérez-Elvira, S., Fdz-Polanco, F., 2015. Simplified mechanistic model for the two-stage anaerobic degradation of sewage sludge. Environmental Technology 36, 1334–1346. https://doi.org/10.1080/09593330.2014.988186

Du, M., Liu, X., Wang, D., Yang, Q., Duan, A., Chen, H., Liu, Y., Wang, Q., Ni, B.-J., 2021. Understanding the fate and impact of capsaicin in anaerobic co-digestion of food waste and waste activated sludge. Water Research 188, 116539. https://doi.org/10.1016/j.watres.2020.116539

EBA (2019), Annual Statistical Report of the European Biogas Association – European Overview 2019. https://www.europeanbiogas.eu/eba-statistical-report-2019 (accessed 03.10.20).

Eberl, H.J., 2003. Simulation of chemical reaction fronts in anaerobic digestion of solid waste, in: Proceedings of the 2003 International Conference on Computational Science and Its Applications: Part I, ICCSA'03. Springer-Verlag, Berlin, Heidelberg, pp. 503–512.

Eberl, H.J., 2005. The role of spatio-temporal effects in anaerobic digestion of solid waste. Nonlinear Analysis: Theory, Methods & Applications, Invited Talks from the Fourth World Congress of Nonlinear Analysts (WCNA 2004) 63, e1497–e1505. https://doi.org/10.1016/j.na.2005.01.045

El-Mashad, H.M., Zhang, R., 2010. Biogas production from co-digestion of dairy manure and food waste. Bioresource Technology 101, 4021–4028. https://doi.org/10.1016/j.biortech.2010.01.027

Fdez.-Güelfo, L.A., Álvarez-Gallego, C., Sales Márquez, D., Romero García, L.I., 2011. Dry-thermophilic anaerobic digestion of simulated organic fraction of Municipal Solid Waste: Process modeling. Bioresource Technology 102, 606–611. https://doi.org/10.1016/j.biortech.2010.07.124

Fedorovich, V., Lens, P., Kalyuzhnyi, S., 2003. Extension of Anaerobic Digestion Model No. 1 with processes of sulfate reduction. Appl Biochem Biotechnol 109, 33–45. https://doi.org/10.1385/abab:109:1-3:33

Froment, G.F., Bischoff, K.B., Wilde, J.D., 2010. Chemical Reactor Analysis and Design, 3rd Edition. John Wiley & Sons, Incorporated.

Harmand, J., Lobry, C., Rapaport, A., Sari, T., 2017. The Chemostat: Mathematical Theory of Microorganism Cultures, Chemical Engineering series / Chemostat and bioprocesses. John Wiley and Sons, Ltd.

Hernández-Shek, M.A., Mathieux, M., André, L., Peultier, P., Pauss, A., Ribeiro, T., 2020. Quantifying porosity changes in solid biomass waste using a disruptive approach of water retention curves (WRC) for dry anaerobic digestion. Bioresource Technology Reports 12, 100585. https://doi.org/10.1016/j.biteb.2020.100585

Holliger, C., Alves, M., Andrade, D., Angelidaki, I., Astals, S., Baier, U., Bougrier, C., Buffière, P., Carballa, M., de Wilde, V., Ebertseder, F., Fernández, B., Ficara, E., Fotidis, I., Frigon, J.-C., de Laclos, H.F., Ghasimi, D.S.M., Hack, G., Hartel, M., Heerenklage, J., Horvath, I.S., Jenicek, P., Koch, K., Krautwald, J., Lizasoain, J., Liu, J., Mosberger, L., Nistor, M., Oechsner, H., Oliveira, J.V., Paterson, M., Pauss, A., Pommier, S., Porqueddu, I., Raposo, F., Ribeiro, T., Rüsch Pfund, F., Strömberg, S., Torrijos, M., van Eekert, M., van Lier, J., Wedwitschka, H., Wierinck, I., 2016. Towards a standardization of biomethane potential tests. Water Sci. Technol. 74, 2515–2522. https://doi.org/10.2166/wst.2016.336

Kalyuzhnyi, S., Veeken, A., Hamelers, B., 2000. Two-particle model of anaerobic solid state fermentation. Water Sci Technol 41, 43–50. https://doi.org/10.2166/wst.2000.0054

Kamali, M., Gameiro, T., Costa, M.E.V., Capela, I., 2016. Anaerobic digestion of pulp and paper mill wastes – An overview of the developments and improvement opportunities. Chemical Engineering Journal 298, 162–182. https://doi.org/10.1016/j.cej.2016.03.119

Kolchanova, E.A., Kolchanov, N.V., 2022. Onset of solutal convection in layered sorbing porous media with clogging. International Journal of Heat and Mass Transfer 183, 122110. https://doi.org/10.1016/j.ijheatmasstransfer.2021.122110

Kouas, M., 2018. Caractérisation cinétique de la biodégradation de substrats solides et application à l'optimisation et à la modélisation de la co-digestion (PhD Thesis). Université Montpellier ; Université de Sfax. Faculté des sciences.

Liotta, F., Chatellier, P., Esposito, G., Fabbricino, M., Frunzo, L., Hullebusch, E.D. van, Lens, P.N.L., Pirozzi, F., 2015. Modified Anaerobic Digestion Model No.1 for dry and semi-dry anaerobic digestion of solid organic waste. Environmental Technology 36, 870–880. https://doi.org/10.1080/09593330.2014.965226

Lovitt, R.W., Wimpenny, J.W.T.Y. 1981, n.d. Physiological Behaviour of Escherichia coli Grown in Opposing Gradients of Oxidant and Reductant in the Gradostat. Microbiology 127, 269–276. https://doi.org/10.1099/00221287-127-2-269

Martin, D.J., Potts, L.G.A., Heslop, V.A., 2003. Reaction Mechanisms in Solid-State Anaerobic Digestion: 1. The Reaction Front Hypothesis. Process Safety and Environmental Protection, Solid Waste Management 81, 171–179. https://doi.org/10.1205/095758203765639870

Müller, T.G., Noykova, N., Gyllenberg, M., Timmer, J., 2002. Parameter identification in dynamical models of anaerobic waste water treatment. Mathematical Biosciences 177–178, 147–160. https://doi.org/10.1016/S0025-5564(01)00098-0

Pastor-Poquet, V., Papirio, S., Harmand, J., Steyer, J.-P., Trably, E., Escudié, R., Esposito, G., 2019. Assessing practical identifiability during calibration and cross-validation of a structured model for high-solids anaerobic digestion. Water Research 164, 114932. https://doi.org/10.1016/j.watres.2019.114932

Rakotoniaina, V.A., 2012. Co-méthanisation des déchets fermiers et alimentaires : expérimentation et modélisation (PhD Thesis). La Réunion.

Ramirez, I., Volcke, E.I.P., Rajinikanth, R., Steyer, J.-P., 2009. Modeling microbial diversity in anaerobic digestion through an extended ADM1 model. Water Research 43, 2787–2800. https://doi.org/10.1016/j.watres.2009.03.034

Rao, M.S., Singh, S.P., Singh, A.K., Sodha, M.S., 2000. Bioenergy conversion studies of the organic fraction of MSW: assessment of ultimate bioenergy production potential of municipal garbage. Applied Energy 66, 75–87. https://doi.org/10.1016/S0306-2619(99)00056-2

Rapaport, A., 2018. Some non-intuitive properties of simple extensions of the chemostat model. Ecological Complexity 34, 111–118. https://doi.org/10.1016/j.ecocom.2017.02.003

Riggio, S., Torrijos, M., Debord, R., Esposito, G., van Hullebusch, E.D., Steyer, J.P., Escudié, R., 2017. Mesophilic anaerobic digestion of several types of spent livestock bedding in a batch leach-bed reactor : substrate characterization and process performance. Waste Management 59, 129–139. https://doi.org/10.1016/j.wasman.2016.10.027

Rocamora, I., Wagland, S.T., Villa, R., Simpson, E.W., Fernández, O., Bajón-Fernández, Y., 2020. Dry anaerobic digestion of organic waste: A review of operational parameters and their impact on process performance. Bioresource Technology 299, 122681. https://doi.org/10.1016/j.biortech.2019.122681

Rouches, E., Escudié, R., Latrille, E., Carrère, H., 2019. Solid-state anaerobic digestion of wheat straw: Impact of S/I ratio and pilot-scale fungal pretreatment. Waste Management 85, 464–476. https://doi.org/10.1016/j.wasman.2019.01.006

Sbarciog, M., Loccufier, M., Noldus, E., 2010. Determination of appropriate operating strategies for anaerobic digestion systems. Biochemical Engineering Journal 51, 180–188. https://doi.org/10.1016/j.bej.2010.06.016

Shewani, A., Horgue, P., Pommier, S., Debenest, G., Lefebvre, X., Gandon, E., Paul, E., 2015. Assessment of percolation through a solid leach bed in dry batch anaerobic digestion processes. Bioresource Technology 178, 209–216. https://doi.org/10.1016/j.biortech.2014.10.017

Simeonov, Iv., Momchev, V., Grancharov, D., 1996. Dynamic modeling of mesophilic anaerobic digestion of animal waste. Water Research 30, 1087–1094. https://doi.org/10.1016/0043-1354(95)00270-7

564 Smith, H.L., Waltman, P., 1995. The Theory of the Chemostat: Dynamics of Microbial Competition. Cambridge
565 University Press. https://doi.org/10.1017/cbo9780511530043

566 Taylor, J.A., Rapaport, A., 2021. Second-order cone optimization of the gradostat. Computers & Chemical
567 Engineering 151, 107347. https://doi.org/10.1016/j.compchemeng.2021.107347

568 van Genuchten, M.Th., Wierenga, P.J., 1976. Mass transfer studies in sorbous porous media I. Analytical solutions.
569 Soil Science Society of America Journal Vol 40.

570 Vavilin, V.A., Rytov, S.V., Lokshina, L.Y., Pavlostathis, S.G., Barlaz, M.A., 2003. Distributed model of solid waste
571 anaerobic digestion: effects of leachate recirculation and pH adjustment. Biotechnology and
572 Bioengineering 81, 66–73. https://doi.org/10.1002/bit.10450

573 Vavilin, V.A., Lokshina, L.Ya., Jokela, J.P.Y., Rintala, J.A., 2004. Modeling solid waste decomposition. Bioresource
574 Technology 94, 69–81. https://doi.org/10.1016/j.biortech.2003.10.034

575 Vavilin, V.A., Angelidaki, I., 2005. Anaerobic degradation of solid material: Importance of initiation centers for
576 methanogenesis, mixing intensity, and 2D distributed model. Biotechnology and Bioengineering 89,
577 113–122. https://doi.org/10.1002/bit.20323

578 Vavilin, V.A., Lokshina, L.Y., Flotats, X., Angelidaki, I., 2007. Anaerobic digestion of solid material:
579 Multidimensional modeling of continuous-flow reactor with non-uniform influent concentration
580 distributions. Biotechnology and Bioengineering 97, 354–366. https://doi.org/10.1002/bit.21239

581 Vavilin, V.A., Fernandez, B., Palatsi, J., Flotats, X., 2008. Hydrolysis kinetics in anaerobic degradation of particulate
582 organic material: An overview. Waste Management 28, 939–951.
583 https://doi.org/10.1016/j.wasman.2007.03.028

584 Velázquez-Martí, B., Meneses-Quelal, O.W., Gaibor-Chavez, J., Niño-Ruiz, Z., 2018. Review of Mathematical
585 Models for the Anaerobic Digestion Process. Anaerobic Digestion.
586 https://doi.org/10.5772/intechopen.80815

587 Xie, S., Lawlor, P.G., Frost, J.P., Hu, Z., Zhan, X., 2011. Effect of pig manure to grass silage ratio on methane
588 production in batch anaerobic co-digestion of concentrated pig manure and grass silage. Bioresource
589 Technology 102, 5728–5733. https://doi.org/10.1016/j.biortech.2011.03.009

590 Xu, F., Wang, Z.-W., Li, Y., 2014. Predicting the methane yield of lignocellulosic biomass in mesophilic solid-state
591 anaerobic digestion based on feedstock characteristics and process parameters. Bioresource
592 Technology 173, 168–176. https://doi.org/10.1016/j.biortech.2014.09.090

593 Xu, F., Li, Y., Wang, Z.-W., 2015. Mathematical modeling of solid-state anaerobic digestion. Progress in Energy and
594 Combustion Science 51, 49–66. https://doi.org/10.1016/j.pecs.2015.09.001

595 Zaher, U., Li, R., Jeppsson, U., Steyer, J.-P., Chen, S., 2009. GISCOD: General Integrated Solid Waste Co-Digestion
596 model. Water Research 43, 2717–2727. https://doi.org/10.1016/j.watres.2009.03.018

Zambrano, J. , Carlsson, B. , 2014. Optimizing zone volumes in bioreactors described by Monod and Contois growth kinetics. In: Proceeding of the IWA World Water Congress & Exhibition, Lisbon, Portugal, p. 6.

Zambrano, J., Carlsson, B., Diehl, S., 2015. Optimal steady-state design of zone volumes of bioreactors with Monod growth kinetics. Biochemical Engineering Journal 100, 59–66. https://doi.org/10.1016/j.bej.2015.04.002

Zhou, L., Selim, H.M., 2001. Solute Transport in Layered Soils. Soil Science Society of America Journal 65, 1056–1064. https://doi.org/10.2136/sssaj2001.6541056x

Zhou, H., Ying, Z., Cao, Z., Liu, Z., Zhang, Z., Liu, W., 2020. Feeding control of anaerobic co-digestion of waste activated sludge and corn silage performed by rule-based PID control with ADM1. Waste Management 103, 22–31. https://doi.org/10.1016/j.wasman.2019.12.021

Figure captions

Fig 1. Schematic representation of the experimentation set up

Fig 2. Schematic representation of the hydrodynamics used in the model

Fig 3. LBR performance on A : accumulated methane yield, B: methane flow and C: VFA concentration for each LBR. Calibration and Validation step on D: accumulated methane yield, E: methane flow and F: VFA concentration; red dots for average experimental values, blue lines for simulated values

Fig 4. A: Monod Kinetic parameters sensitivity for methane flow, B: Haldane Kinetic parameters sensitivity for methane flow

Fig 5. Absolute sensitivity of kinetic parameters as a function of time for A : accumulated methane yield, B: methane flow, and C: VFA concentration.

Fig 6. Solutes concentrations inside mobile (A) and immobile (B) regions

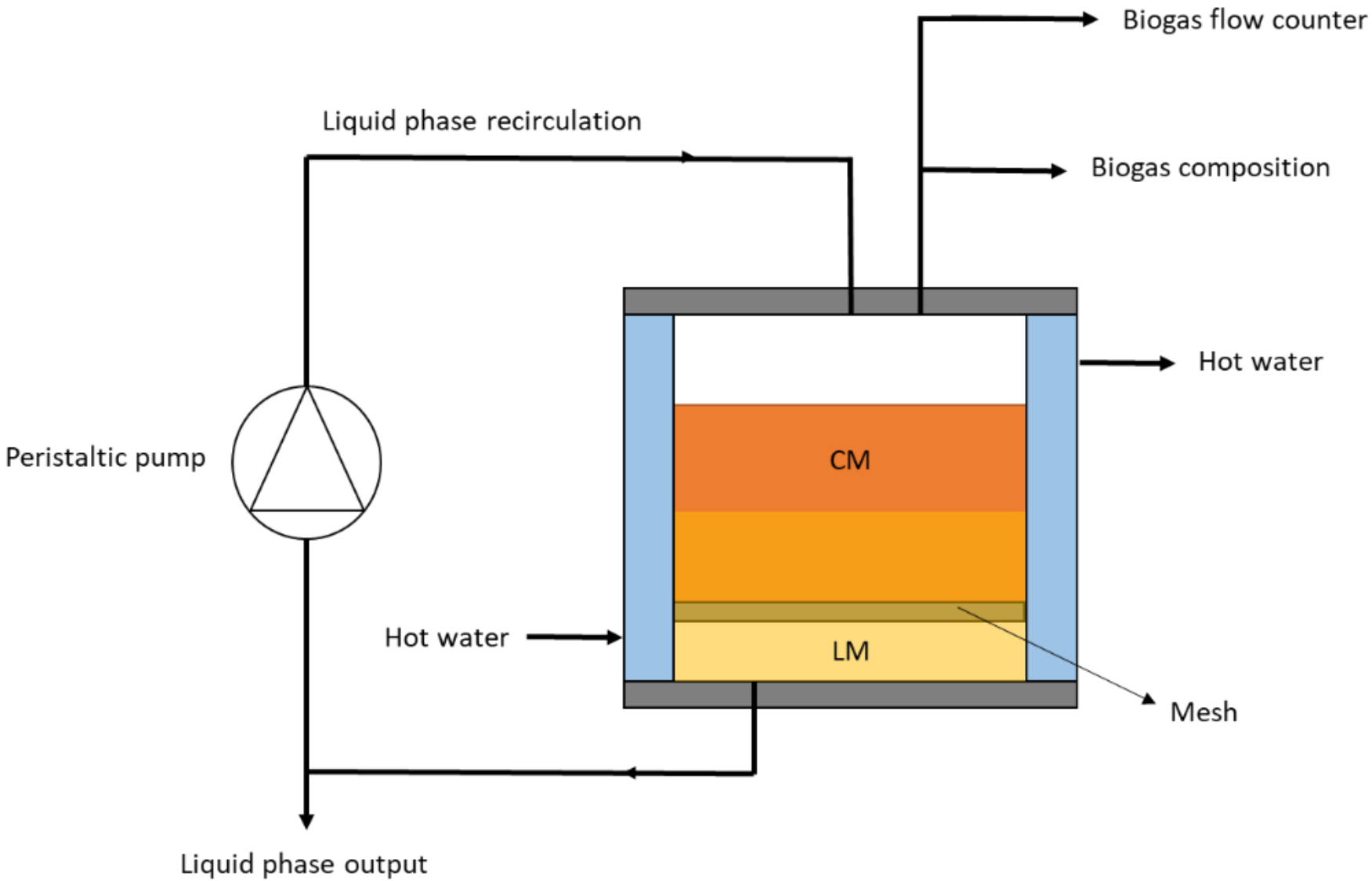
Biogas flow counter
Liquid phase recirculation
Biogas composition
Hot water
Peristaltic pump
CM
Hot water
LM
Mesh
Liquid phase output

Mobile-Immobile water model

$$\theta_m + \theta_{im} = 1$$

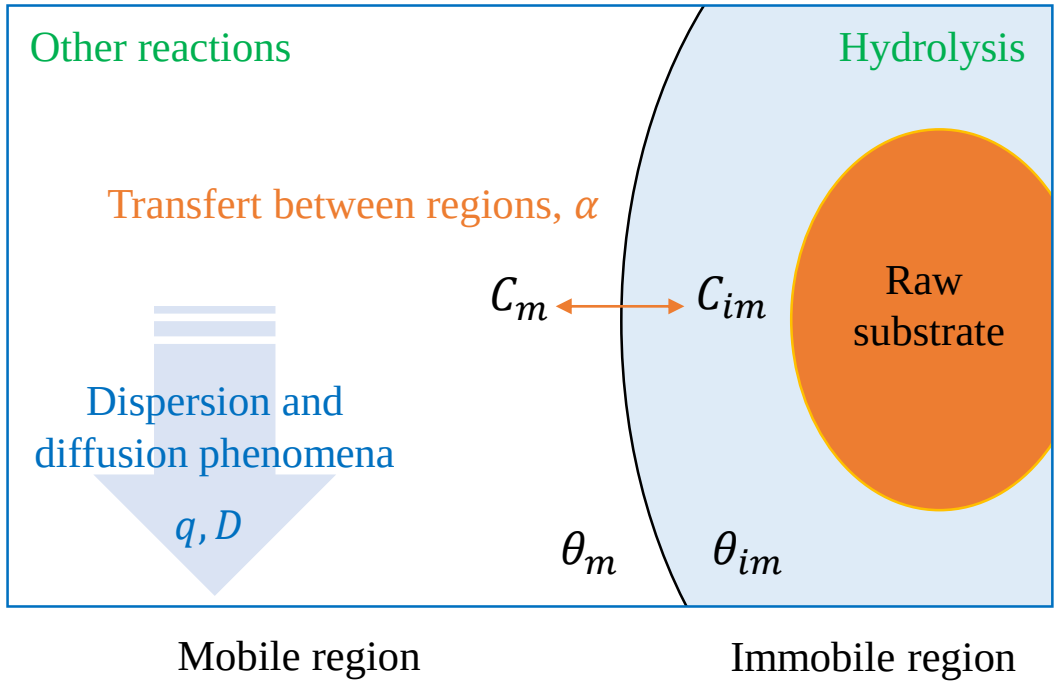

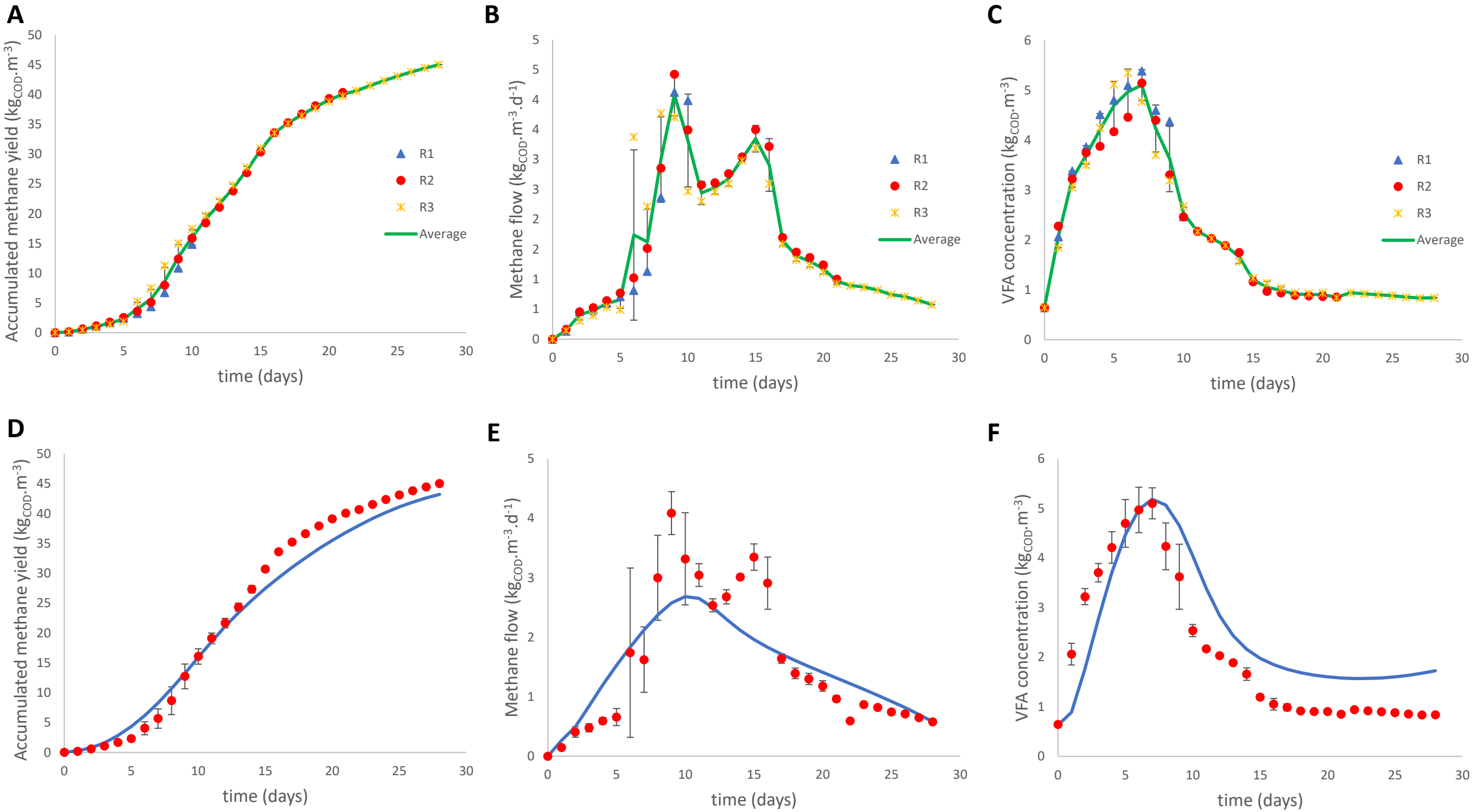
A
Accumulated methane yield (kgCOD.m-3)
time (days)
R1
R2
R3
Average
B
Methane flow (kgCOD.m-3.d-1)
time (days)
R1
R2
R3
Average
C
VFA concentration (kgCOD.m-3)
time (days)
R1
R2
R3
Average
D
Accumulated methane yield (kgCOD.m-3)
time (days)
E
Methane flow (kgCOD.m-3.d-1)
time (days)
F
VFA concentration (kgCOD.m-3)
time (days)

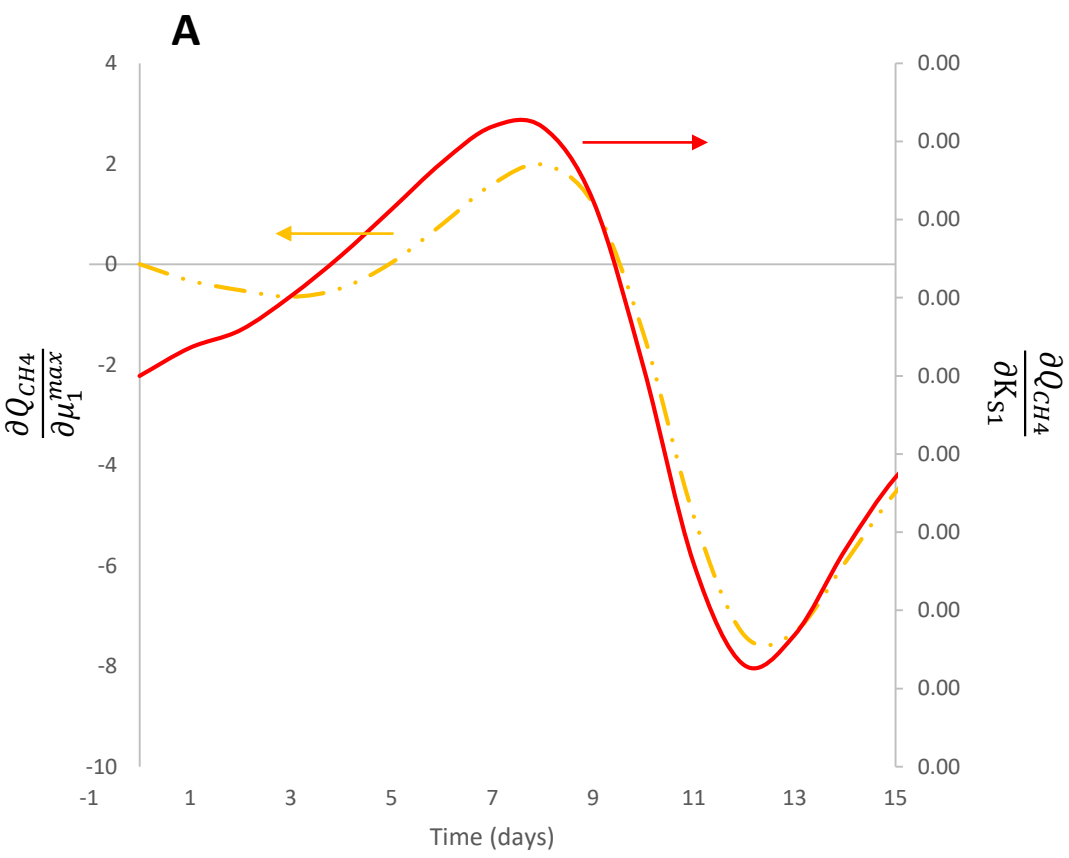
A
4
2
0
-2
-4
-6
-8
-10
-1
1
3
5
7
9
11
13
15
Time (days)
0.00
$\frac{\partial Q_{CH4}}{\partial \mu_1^{max}}$
$\frac{\partial Q_{CH4}}{\partial K_{S1}}$

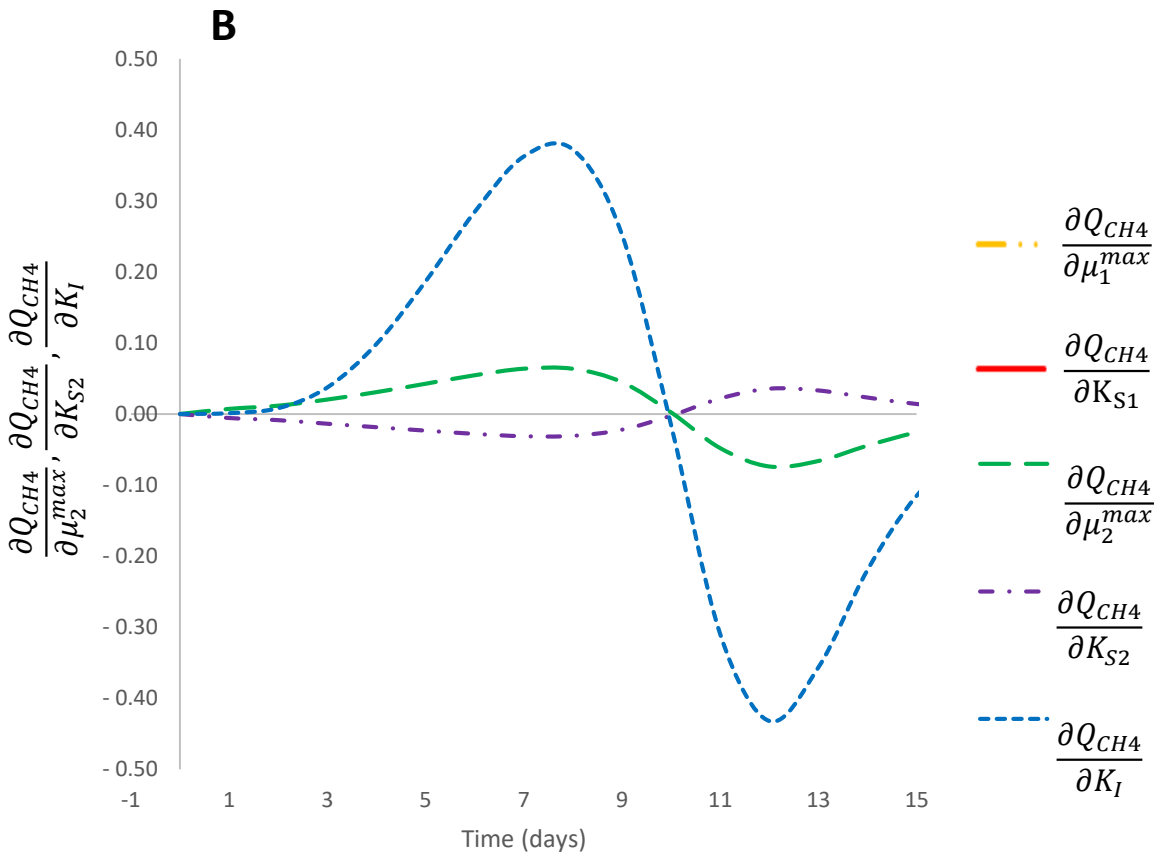
B
0.50
0.40
0.30
0.20
0.10
0.00
- 0.10
- 0.20
- 0.30
- 0.40
- 0.50
-1
1
3
5
7
9
11
13
15
Time (days)
$\frac{\partial Q_{CH4}}{\partial \mu_2^{max}}, \frac{\partial Q_{CH4}}{\partial K_{S2}}, \frac{\partial Q_{CH4}}{\partial K_I}$
$\frac{\partial Q_{CH4}}{\partial \mu_1^{max}}$
$\frac{\partial Q_{CH4}}{\partial K_{S1}}$
$\frac{\partial Q_{CH4}}{\partial \mu_2^{max}}$
$\frac{\partial Q_{CH4}}{\partial K_{S2}}$
$\frac{\partial Q_{CH4}}{\partial K_I}$

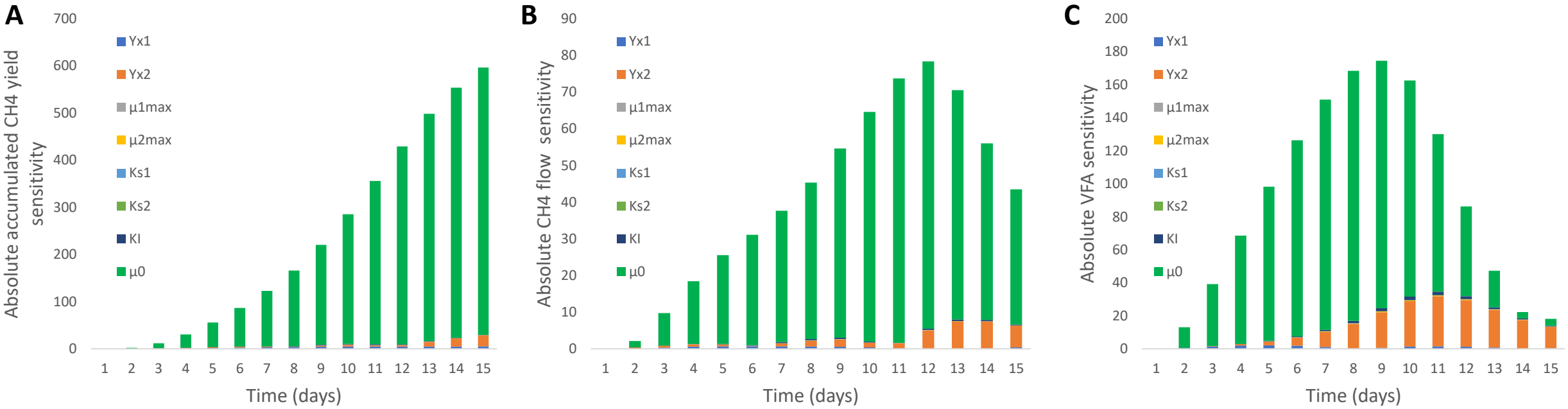
A
Absolute accumulated CH4 yield sensitivity
700
600
500
400
300
200
100
0
Yx1
Yx2
µ1max
µ2max
Ks1
Ks2
KI
µ0
1 2 3 4 5 6 7 8 9 10 11 12 13 14 15
Time (days)
B
Absolute CH4 flow sensitivity
90
80
70
60
50
40
30
20
10
0
Yx1
Yx2
µ1max
µ2max
Ks1
Ks2
KI
µ0
1 2 3 4 5 6 7 8 9 10 11 12 13 14 15
Time (days)
C
Absolute VFA sensitivity
200
180
160
140
120
100
80
60
40
20
0
Yx1
Yx2
µ1max
µ2max
Ks1
Ks2
KI
µ0
1 2 3 4 5 6 7 8 9 10 11 12 13 14 15
Time (days)

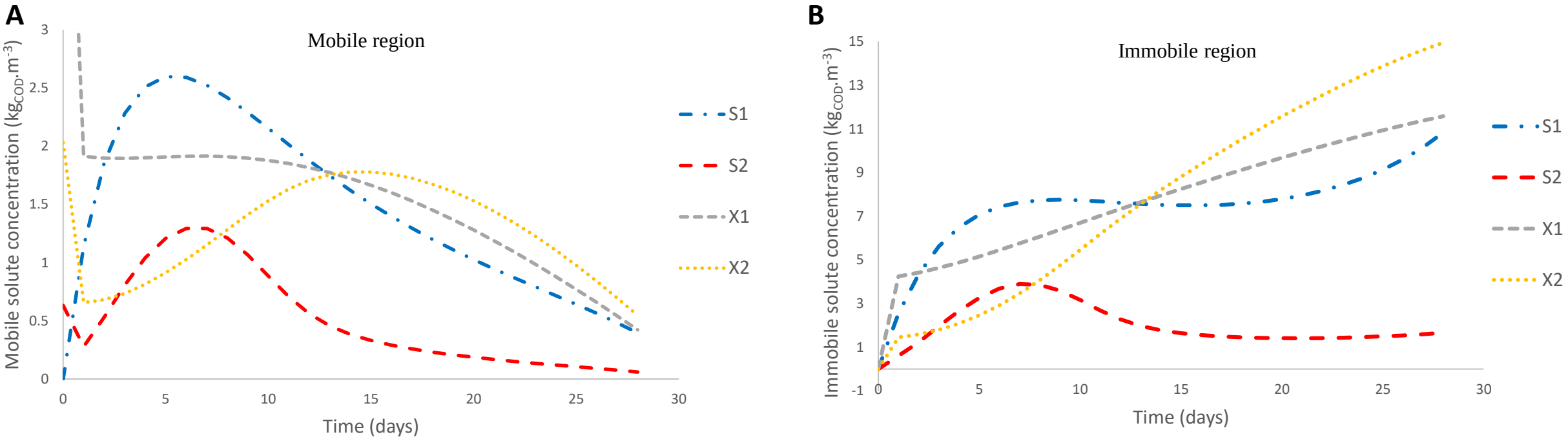
A
Mobile region
Mobile solute concentration (kg$_{COD}$.m^{-3})
3
2.5
2
1.5
1
0.5
0
0
5
10
15
20
25
30
Time (days)
S1
S2
X1
X2
B
Immobile region
Immobile solute concentration (kg$_{COD}$.m^{-3})
15
13
11
9
7
5
3
1
-1
0
5
10
15
20
25
30
Time (days)
S1
S2
X1
X2

Table 1 Chemical characteristics of inoculum and initial substrate used

	TS	**VS**	**pH**	**FOS**	**TAC**	**BMP***
	%	$\%_{TS}$	-	$mg.L^{-1}$	$mg.L^{-1}$	$NL.kg_{VS}^{-1}$
Initial CM	22.0 ± 0.01	87.7 ± 0.01	7.51 ± 0.01	-	-	222.8 ± 4.4
Initial LM	1.61 ± 0.01	62.7 ± 0.01	7.92 ± 0.01	96.81 ± 5.5	3460 ± 62	10.4 ± 0.01

*grinded and mixed with GM 200 Retsch, Germany

Table 2 Hydrodynamic parameters

Time (day)	$\theta(\%)$	$\theta_m(\%)$	$\theta_{im}(\%)$
0	91.02±0.23	30.53±2.49	60.49±2.29
10	91.83±0.38	18.86±2.76	72.97±2.38
15	90.02±0.03	14.80±2.75	75.22±2.78
21	91.99±0.11	08.64±0.84	83.35±0.96
31	90.03±0.17	01.62±0.28	88.41±0.45

Table 3 Peterson matrix of the simplified three-reaction mechanistic model

Step	S_0	S_1	S_2	X_1	X_2	CH_4	Reaction rate
Hydrolysis	-1	1					$r_0 = \mu_0 S_0$
Acidogenesis		-1	$(1 - Y_{X1})$	Y_{X1}			$r_1 = \mu_1^{max} \frac{S_1 X_1}{S_1 + K_{S1}}$
Methanogenesis			-1		Y_{X2}	$(1 - Y_{X2})$	$r_2 = \mu_2^{max} \frac{S_2 X_2}{S_2 + K_{S2} + \frac{S_2^2}{K_I}}$

Table 4 Peterson matrix of the model used

Step	S_0	S_1^m	S_1^{im}	X_1^m	X_1^{im}	S_2^m	S_2^{im}	X_2^m	X_2^{im}	CH_4	**Reaction rate**
Hydrolysis	-1	f_{m0}	$(1-f_{m0})$								$r_0 = \mu_0 S_0$
Acidogenesis											
Mobile region		-1		Y_{X1}		$(1-Y_{X1})$					$r_1^m = \mu_1^{max} \frac{S_1^m X_1^m}{S_1^m + K_{S1}}$
Stagnant region			-1		Y_{X1}		$(1-Y_{X1})$				$r_1^{im} = \mu_1^{max} \frac{S_1^{im} X_1^{im}}{S_1^{im} + K_{S1}}$
Methanogenesis											
Mobile region						-1		Y_{X2}		$(1-Y_{X2})$	$r_2^m = \mu_2^{max} \frac{S_2^m X_2^m}{S_2^m + K_{S2} + \frac{(S_2^m)^2}{K_I}}$
Stagnant region							-1		Y_{X2}	$(1-Y_{X2})$	$r_2^{im} = \mu_2^{max} \frac{S_2^{im} X_2^{im}}{S_2^{im} + K_{S2} + \frac{(S_2^{im})^2}{K_I}}$

Table 5 Initialization values for kinetic parameters

Parameter	Initialization value	Interval	Unit
Y_{X1}	0.0264	[0.01 – 0.3]	$-$
Y_{X2}	0.0264	[0.01 – 0.3]	$-$
μ_1^{max}	0.4	[0.1 – 30]	d^{-1}
μ_2^{max}	0.4	[0.1 – 30]	d^{-1}
K_{S1}	160	[10 – 1000]	$g_{COD}.L^{-1}$
K_{S2}	0.82	[0.1 – 120]	$g_{COD}.L^{-1}$
K_I	41.85	[0.1 – 50]	$g_{COD}.L^{-1}$

Table 6 Kinetic parameters estimation

Parameter	Unit	Value
Y_{X1}	-	0.0928
Y_{X2}	-	0.2376
μ_1^{max}	d^{-1}	29.998
μ_2^{max}	d^{-1}	29.959
K_{S1}	$g_{COD}.L^{-1}$	165.41
K_{S2}	$g_{COD}.L^{-1}$	37.883
K_I	$g_{COD}.L^{-1}$	1.5385
iterations	-	150
SD	$g_{COD}.L^{-1}$	77.777

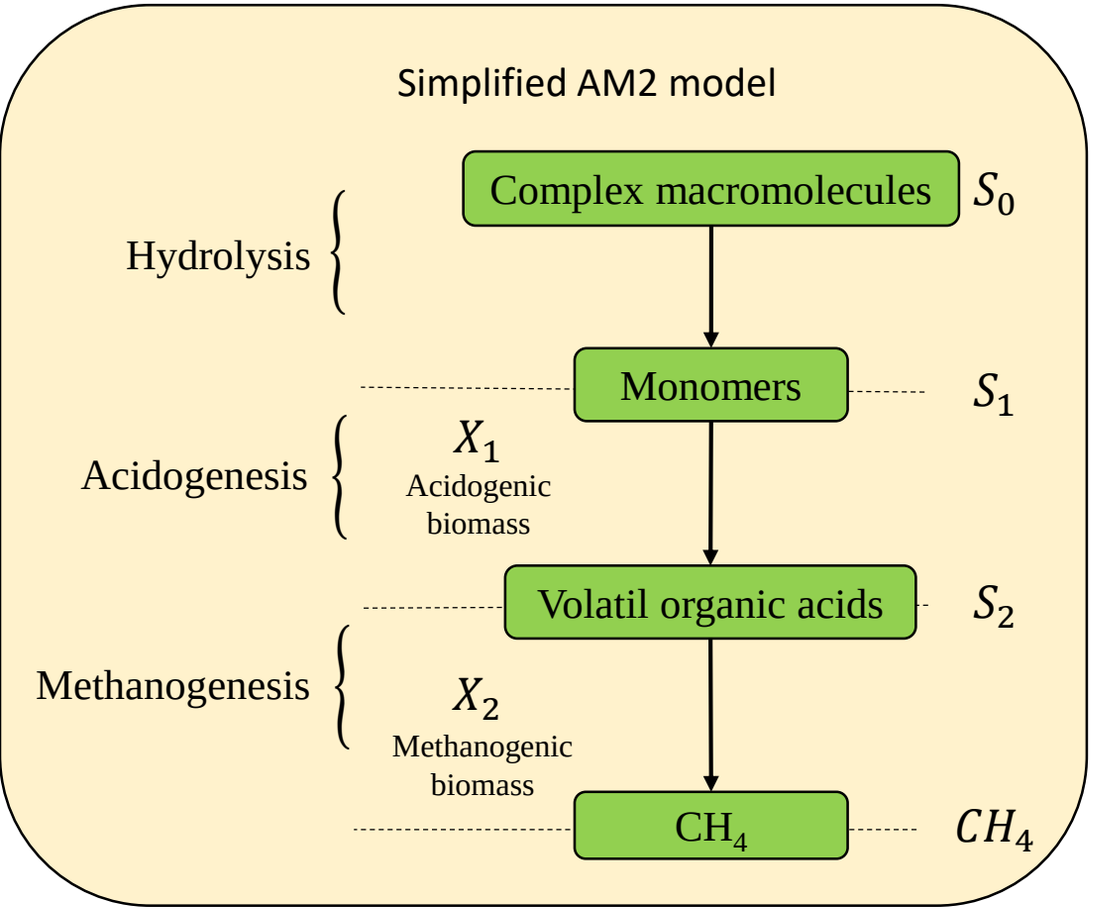

Mobile-Immobile water model

$$\theta_m + \theta_{im} = 1$$